



A Strategy for a Routine Pattern Informatics Operation Applied to Taiwan

LING-YUN CHANG,¹ CHIEN-CHIH CHEN,¹ YI-HSUAN WU,¹ TZU-WEI LIN,² CHIEN-HSIN CHANG,² and CHIH-WEN KAN²

Abstract—We systematically investigated precursory seismic patterns using the pattern informatics (PI) method and suggest an operable procedure for making PI maps for all seasons, in the context of earthquake forecasting. We examined the PI patterns before several inland earthquakes with magnitudes larger than 6, which occurred between 2001 and 2010 in Taiwan. We fixed a cutoff magnitude and a change interval, which is the time span used to calculate the seismicity change. Our results show that locations with high PI anomalies are typically associated with large earthquakes when the cutoff magnitude is 3.2 and the change interval is 4 years. Therefore, the PI method can be utilized as a routine forecasting tool with regular updates, such performing the PI calculation every season. We also conducted random tests, the results of which indicate a significant difference between large events and random, hypothetical events.

Key words: Pattern informatics, earthquake forecasting, phase dynamics, Taiwan seismicity.

1. Introduction

Spatiotemporal seismicity is related to crustal stresses and stress fields that change complexly over various scales of time and space. The occurrence of a large earthquake may be related to the critical stress threshold of a fault plane (CHEN *et al.* 2006b). Thus, detecting whether unusual seismicity occurs before a large earthquake has been proposed as the foundation of earthquake prediction in many studies (TIAMPO and SHCHERBAKOV 2012). This study focuses on pattern informatics, as a branch of earthquake prediction algorithms. Pattern informatics (PI) originated from RUNDLE *et al.* (2000) and has been further developed

by TIAMPO *et al.* (2002), NANJO *et al.* (2006), HOLLIDAY *et al.* (2007) and WU *et al.* (2008b) over the past decade. Pattern informatics describes anomalous changes in seismicity (CHEN *et al.* 2005; TIAMPO *et al.* 2002), including activation and quiescence, as a point process in a phase dynamical system. The spatiotemporal evolution of the dynamical system can be characterized by the phase drift. In pattern informatics, the phase drift can be quantified by calculating the seismic activity over a period of time, termed the change interval, and normalizing over the background seismicity.

We applied pattern informatics to the retrospective analyses of several earthquakes with magnitudes greater than 6 and depths shallower than 25 km, which occurred on Taiwan Island from 2001 through 2010. The results of these retrospective pattern informatics analyses allowed further insight into the standard procedure of the routine operation of pattern informatics forecasting. We also randomized the PI parameters, including the cutoff magnitude and the duration of change interval, to examine the significance of PI forecasts.

2. Methods

Pattern informatics can describe changes in seismicity through a phase dynamical system. Changes in seismicity over time are associated with rotations of the state vector in Hilbert space. Stress accumulation and release cause the state vector in the phase dynamical space of the seismic system to change. Excepting the normalized length of the state vector, all information related to a change in the dynamical system can be described by the rotation of the phase angle. Thus, pattern informatics uses the phase drift to express the spatial and temporal

¹ Graduate Institute of Geophysics and Department of Earth Sciences, National Central University, Jhongli 32001, Taiwan, ROC. E-mail: maomaowyh@gmail.com; yhwu@ncu.edu.tw

² Seismological Center, Central Weather Bureau, Taipei 10048, Taiwan, ROC.

evolution of the dynamical system. Pattern informatics calculates the angle of drift over a period of time, the change interval, to predict whether the area is at seismic risk in the coming period of time, the predict interval.

The procedures for the PI method are described as follows:

1. The study area is binned into many grids of size $0.1^\circ \times 0.1^\circ$.
2. Four time parameters are defined. First, t_0 denotes the beginning time of the catalog. Second, t_1 and t_2 mark the start and end of the change interval, respectively. Finally, a sampling reference time, t_b , shifts between t_0 and t_1 . The t_b is shifted by 3 days to remove some of the clustering after-shock and background fluctuations.
3. The seismic intensity, $I(x_i, t_b, t)$ is defined as the average number of earthquakes between t_b and t with magnitudes larger than the cutoff magnitude, M_C , that occur in the grid box, x_i , and its eight neighboring boxes. Thus, the change in intensity during the change interval, i.e., $\Delta I(x_i, t_b, t_1, t_2) = I(x_i, t_b, t_1) - I(x_i, t_b, t_2)$, can be computed, and is denoted by $\Delta I(x_i, t_b)$.
4. For each x_i , shifting by t_b produces a time series of $\Delta I_{x_i}(t_b)$. We then perform a temporal normalization and obtain a temporally normalized intensity change, $\tilde{\Delta I}_{x_i}(t_b)$, for each location, x_i . After temporal normalization, we spatially normalize the spatial series for each t_b to obtain a spatio-temporally normalized intensity change $\hat{\Delta I}_{x_i}(x_i, t_b)$.
5. The normalized intensity change, $\hat{\Delta I}_{x_i}(x_i, t_b)$, is computed at each location. To consider both activation and quiescence, we take the absolute value of the change. The temporal average of $|\hat{\Delta I}_{x_i}(x_i, t_b)|$, denoted by $|\overline{\hat{\Delta I}}(x_i)|$, is then computed for each location. Finally, the mean squared change, $P(x_i) = \overline{|\hat{\Delta I}(x_i)|^2}$, which indicates the relative possibility of large-threshold events, is computed.
6. In a PI map, the mean-subtracted index of the probability of occurrence, i.e., $\Delta P(x_i) = P(x_i) - \mu_P$, is color-coded and plotted. Here, μ_P is the mean of $P(x_i)$ over all boxes and can be considered to be the average background probability for the entire area.

3. Data

In this study, we analyzed the data catalog from the Central Weather Bureau Seismic Network (CWBSN) in Taiwan. The CWBSN has been responsible for monitoring regional seismic activity since 1991. It currently consists of a central recording system with 71 telemeter stations, which are equipped with 3-component Teledyne/Geotech S13 seismometers. The CWBSN has had enhanced earthquake monitoring capability in Taiwan since the end of 1993 (WU and CHIAO 2006, WU *et al.* 2008b). Figure 1 shows the distribution of earthquake depth versus time. The plot shows a considerable increase in the number of earthquakes after 1994. Therefore, considering the consistency of the earthquake catalog, we set 01/01/1994 as the starting point of the data, t_0 . In Fig. 1, we denote the large earthquakes, those with a magnitude larger than 6, which occurred from 2001 to 2010 with red circles, and those before 2001 with white circles.

The ratio of the cumulative number of earthquakes shallower than a given depth to the total number of earthquakes is shown in Fig. 2. We see that approximately 80 % of total earthquakes occur above a depth of 25 km. Therefore, for analyzing the seismicity change using the PI method, we chose earthquakes with depths less than 25 km within Taiwan and within 20 km of its coastline to account for the location error (the yellow area in Fig. 3). There are 539 study cells shown in Fig. 3. To investigate the precursors of large earthquakes, we used earthquakes with magnitudes larger than 6 and depths less than 25 km from 2001 to 2010. There is a total of 7 of these, which represent the target earthquakes in this study (Table 1; Fig. 3, red circles).

The end of the change interval, t_2 , is defined as the end of the last season before each target earthquake. For instance, if the target earthquake occurred on 12/10/2003, t_2 should be 09/30/2003. Based on prior experience, we set the change interval to 4 years, so t_1 is 4 years before t_2 .

A cutoff magnitude (M_C) is given to confirm the quality of data. Earthquakes with magnitudes smaller than the cutoff magnitude were not considered in the calculation. According to previous studies (CHEN

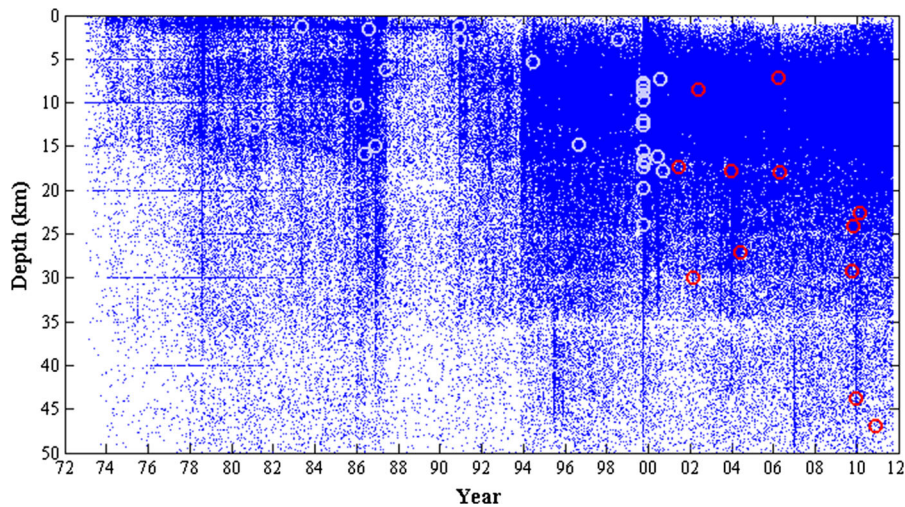


Figure 1

The distribution of earthquake depth versus time. The distribution shows an increase in the number of earthquakes after 1994. The white circles indicate earthquakes with magnitudes larger than 6 before 2001. The red circles indicate earthquakes with magnitudes larger than 6 from 2001 to 2010, and 7 red circles are at depths shallower than 25 km

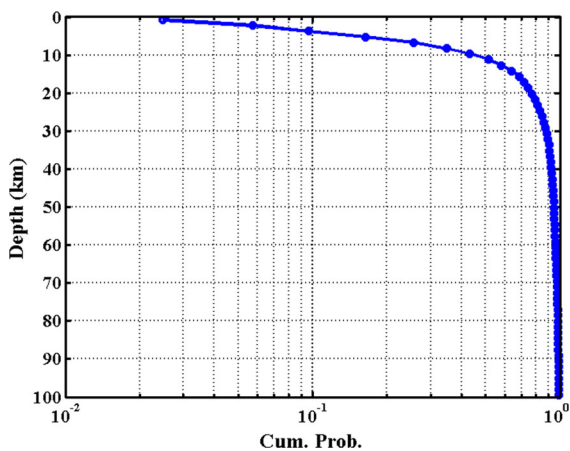


Figure 2

The ratio of the cumulative number of earthquakes that occurred at depths shallower than each given depth, to the total number of earthquakes. Eighty percent of earthquakes occur above 25 km

et al. 2005, 2006a; WU et al. 2008a, b; MIGNAN et al. 2011), we use $M_C = 3.2$ for this study.

4. Results

In our study, we chose 7 target earthquakes (Table 1) to investigate the precursor phenomena. Figure 4 is the hotspot map for the December 10, 2013 Chengkung earthquake (the third one in

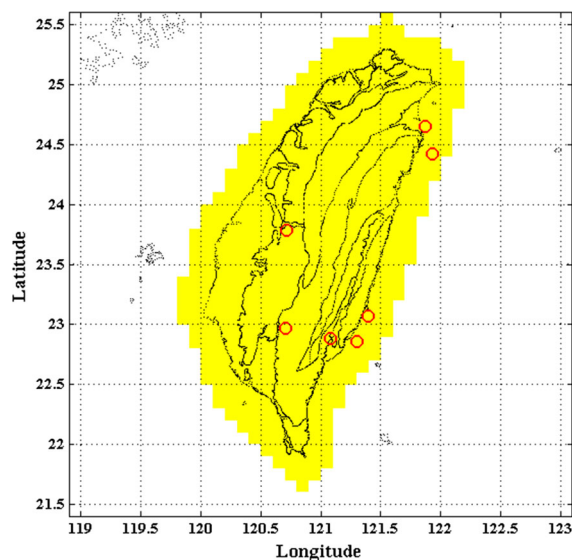


Figure 3

The study area. The yellow grid indicates the area analyzed in PI calculations. The red circles indicate the epicenters of the 7 target events

Table 1), which had a magnitude of 6.4 and hypocenter depth of 17.7 km. We colored the 100 boxes with the highest PI values, with darker colors representing higher values. We plotted blue circles to indicate the epicenter of the Chengkung earthquake, and inverted gray triangles for the locations of earthquakes with magnitudes larger than 5.5 that

Table 1
Parameters of the 7 target events in this study

| # | Longitude | Latitude | Year | Month | Day | Depth | M_W | t_1 | t_2 | M_C | % |
|---|-----------|----------|------|-------|-----|-------|-------|------------|------------|-------|----|
| 1 | 121.9280 | 24.4188 | 2001 | 6 | 14 | 17.29 | 6.30 | 1997/3/31 | 2001/3/31 | 3.2 | 61 |
| 2 | 121.8718 | 24.6510 | 2002 | 5 | 15 | 8.52 | 6.20 | 1998/3/31 | 2002/3/31 | 3.2 | 91 |
| 3 | 121.3982 | 23.0667 | 2003 | 12 | 10 | 17.73 | 6.42 | 1999/9/30 | 2003/9/30 | 3.2 | 88 |
| 4 | 121.0807 | 22.8835 | 2006 | 4 | 1 | 7.20 | 6.23 | 2001/12/31 | 2005/12/31 | 3.2 | 85 |
| 5 | 121.3035 | 22.8555 | 2006 | 4 | 15 | 17.90 | 6.04 | 2002/3/31 | 2006/3/31 | 3.2 | 87 |
| 6 | 120.7187 | 23.7890 | 2009 | 11 | 5 | 24.08 | 6.15 | 2005/9/30 | 2009/9/30 | 3.2 | 42 |
| 7 | 120.7066 | 22.9691 | 2010 | 3 | 4 | 22.64 | 6.42 | 2005/12/31 | 2009/12/31 | 3.2 | 94 |

Time t_2 is the final day of the last season before the earthquake occurred, and time t_1 is 4 years before t_2 , when we set the fixed change interval M_C is the cutoff magnitude, from which we calculate the PI hotspot map using fixed parameters, and the percentile (%) is the percentage of the PI value of the epicenter for the entire map

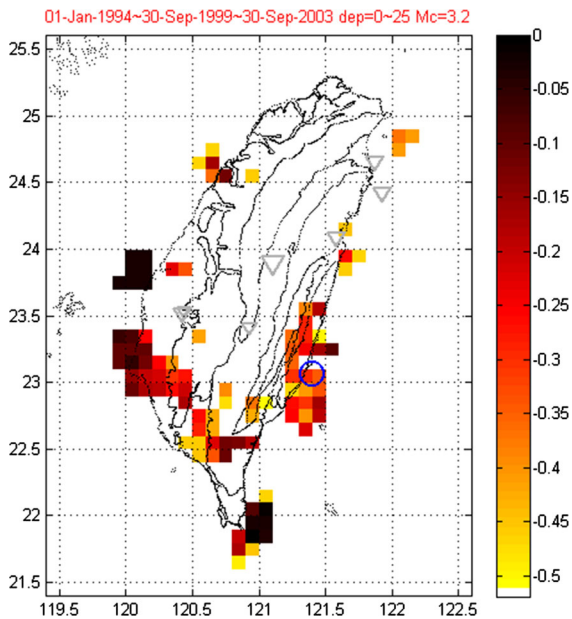


Figure 4

The hotspot map from the Chengkung earthquake (121.40°E, 23.07°N), which occurred on 12/10/2003. The 100 boxes with the highest PI value are colored, with darker colors indicating higher values. The blue circles indicate the locations of earthquakes with magnitudes larger than 5.5 in the prediction interval. The inverted triangle indicates the location of earthquakes with magnitudes larger than 5.5 in the change interval

occurred during the change interval from September 30, 1999 to September 30, 2003. The epicenter of the Chengkung earthquake is located in an anomalously high-PI area. However, a weakness of the current hotspot map is that it is noisy. The noise is most likely caused by a single event throughout the

discretized temporal windows and lacks statistical significance.

Using the same process, we can produce hotspot maps of other target earthquakes. Figure 5a is the hotspot map for the first target earthquake, which occurred on 6/14/2001 and had a magnitude of 6.3 and hypocenter depth of 17.3 km. Figure 5a shows that there are many anomalies in southern Taiwan, although the target epicenter (121.93°E, 24.42°N) is located near an anomalous area. Figure 5b is the hotspot map for the second target earthquake (121.87°E, 24.65°N), which occurred on 5/15/2002, and had a magnitude of 6.2 and hypocenter depth of 8.5 km. The epicenter was formed with a high PI anomaly before the target event. Additionally, when compared to Fig. 4, we notice that the anomalously high-PI area that appeared during the Chengkung earthquake, 4 years earlier, migrated from the surroundings to the center. This migration is similar to that of the 1999 Chi-Chi earthquake and the 2006 Pingtung earthquake (Wu *et al.* 2008a, b, 2011).

Figure 5c is the hotspot map for the fourth target earthquake (121.08°E, 22.88°N), which occurred on 4/1/2006 in Taitung and had a magnitude of 6.2 and hypocenter depth of 7.2 km. Fifteen days later, this area experienced another earthquake (121.30°E, 22.86°N) with a magnitude larger than 6, which occurred on 4/15/2006 and had a hypocenter depth of 17.9 km. Per the operational definition, both events share the same PI hotspot map. However, we are curious about what caused the PI map to have a

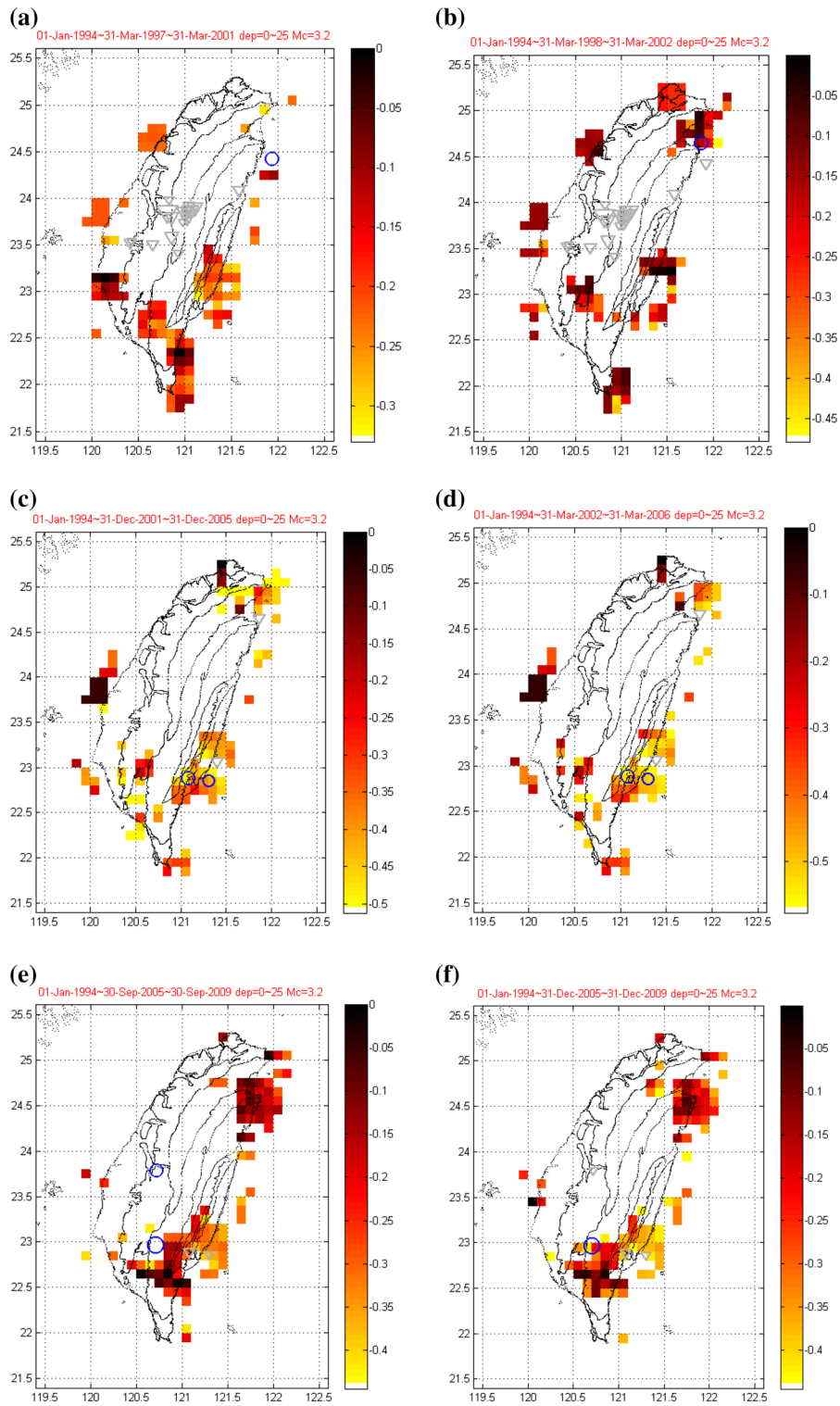


Figure 5

The hotspot maps from the other six target events. The symbols are the same as in Fig. 4. The hotspot map from a the first, b the second, c the fourth, d the fifth, e the sixth and f the seventh target event

slightly downward-shifted change interval, as shown in Fig. 5d. The patterns of Fig. 5c, d are very similar, and both epicenters are located in the anomalously high-PI area.

Figure 5e is the hotspot map for the sixth target earthquake (120.72°E, 23.79°N), which occurred on 11/5/2009, and had a magnitude of 6.1 and hypocenter depth of 24.08 km. The anomalies are distributed in the northeast and southern parts of Taiwan, and the epicenter is located outside the anomalous area. The anomalies may be strongly associated with the southern area where the Jiasian earthquake, the seventh target earthquake, occurred. It had a magnitude of 6.4 on March 4, 2010. Figure 5f is the PI hotspot map for the Jiasian earthquake (120.71°E, 22.97°N), with a hypocenter depth of 22.6 km.

After analyzing all 7 target earthquakes listed in Table 1, we have evidence that the anomalous locations that resulted from the PI calculations are closely associated with earthquakes. It is best to monitor anomalous areas for approximately 4 years, constituting the change interval, before an earthquake. Therefore, the results suggest a standard PI-forecasting process to regularly examine the anomalous areas, which may be potentially associated with high seismic risks in the future.

5. Discussion and Random Test

To confirm the statistical significance of the above PI calculation, we performed three random tests under different conditions. Because the range of PI values in each PI hotspot map may vary, we express the PI value by percentile in the following random tests.

In the first test, we examined the sensitivity of the PI index to the times and locations of target earthquakes by picking 7 PI indices at different times and locations. We also examined the reality of the PI index, that is, whether the PI index reflects the anomalous seismicity, by randomizing the catalog.

To examine whether the PI index occurred around the target earthquakes, we randomly picked 10,000 times between 01/01/2000 and 09/30/2011, at 10,000 locations in our study region. To avoid the effect of large, target events in Table 1, we blanked out the

locations with distances to the epicenter of target earthquakes shorter than 0.5°, as well as the times preceding target events within 1 year when sampling the 10,000 random points. The blue dots in Fig. 6 show the 10,000 randomly chosen times and their spatial grid numbers. We consider the randomly chosen times and locations to be imaged events, for comparing with target events, and call them “random events” after comparison. The red stars indicate the 7 target large events, which, by definition, are associated with a blank area both near and before them. Among the 10,000 random events, we randomly chose 7, for which we calculated the PI hotspot maps using fixed PI parameters ($M_C = 3.2$ and 4 years for the change interval). The cumulative probability of the PI index for the 7 random events is shown as the black line in Fig. 9.

Figure 7 is the normalized hotspot map of the Chengkung earthquake. We only colored those cells with percentiles larger than the Chengkung epicenter. Because the percentile at the epicenter of the Chengkung earthquake is approximately 0.9, there are approximately 60 colored cells. Figure 8 shows the hotspot maps of other target earthquakes, recolored by percentile. The percentile of each target earthquake is also shown in the last column of Table 1. The percentiles of large target events are

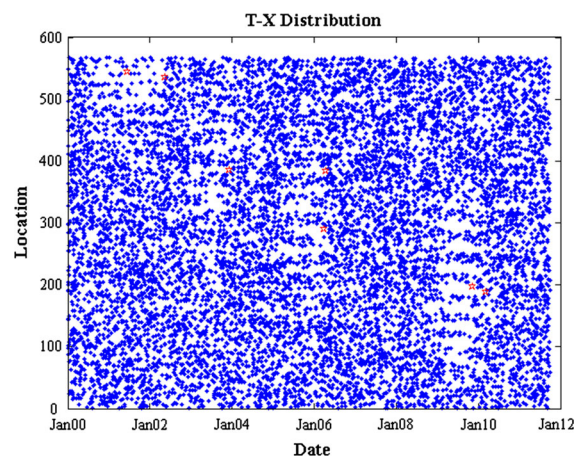


Figure 6

The 10,000 imaged events, shown over time, versus cell numbers. We call them “random events.” The blue dots represent the random events, whose occurrence in time and space are chosen randomly. The red stars indicate the target events. Random events that are near and before the target events are removed to eliminate the effects of the target events

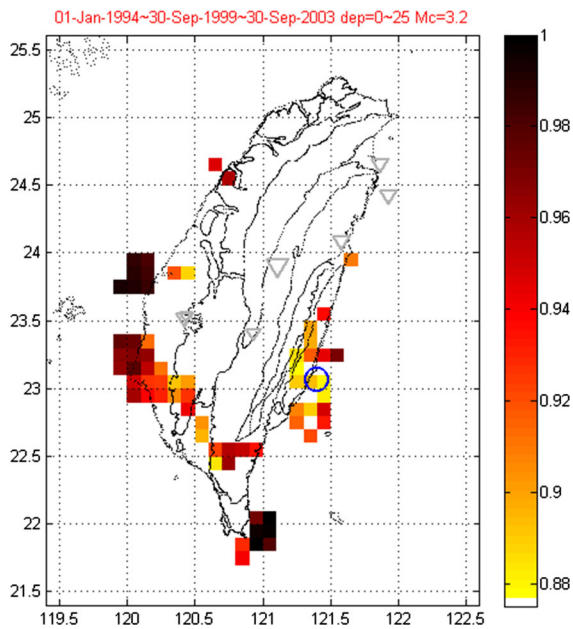


Figure 7

The hotspot map of the Chungkung earthquake that occurred on 12/10/2003, recolored by percentile. Cells with percentiles larger than that of the epicenter are colored

typically high and, therefore, the cumulative probability curve of these 7 target events, represented by the blue line in Fig. 9, is initially flat but quickly increases after percentile 0.8.

In order to show that the PI indices reflect the seismic anomalies, we randomized the location of the data using the Poisson model, with the 7 target earthquakes unchanged. First, we counted the number of events for each grid from the real data set and calculated the mean value. Then, we gave event numbers to each grid, which followed the Poisson distribution. Finally, we kept the times of the original data set, but randomly picked a location from the last step. The red line in Fig. 9 shows the cumulative probability for the 7 target earthquakes with randomized data. The cumulative probability for the 7 random events (black line in Fig. 9), as well as that for the 7 target earthquakes with randomized data (red line in Fig. 9), trend diagonally. This denotes that high and low PI values are chosen approximately equally often in these two cases. Accordingly, the Kolmogorov–Smirnov test concludes that the high-quality performance of the PI forecasts for those 7 large target events was not obtained by chance.

In the second test, we wanted to confirm the effect of the chosen parameters, cutoff magnitude and length of the change interval. We made PI hotspot maps for 7 target events, and 20 random events, using random PI parameters. For this analysis, M_C was chosen between 3 and 4, and the length of the change interval was chosen between 1 and 5 years. For each event, 10,000 PI hotspot maps with different parameters were generated, and the PI percentiles of each event were calculated. These parameters may affect the PI hotspot map and hence the probability distribution of PI percentiles. As an example, Fig. 10 shows the probabilities of the percentiles for the Chengkung earthquake. The percentiles of the Chengkung earthquake in the 10,000 PI hotspot maps, which are generated with different parameters, cluster at approximately 0.9 and 0.72. The blue arrow indicates the result from the fixed parameter analysis, 3.2 for M_C and 4 years for the change interval. We sum the probability to obtain the cumulative curve shown in Fig. 11. The cumulative curves of 7 target events are shown by the gray and black lines in Fig. 11, while the solid circles indicate the results from the fixed parameters for every target. All 7 cumulative curves occur in the area between the diagonal line and the lower right corner, and the probabilities of having percentiles larger than 60 % at the epicenter are above 0.6 for all 7 target earthquakes. Conversely, the average of the results, which is calculated 10,000 times for each of the 20 random events, is shown by blue line, with the light blue dashed lines representing one standard deviation of the percentile. Although the blue curve is initially flat, it increases linearly from 0.2 to 0.8 and becomes flat again at the end. The curve is almost diagonal, indicating a uniform percentile. All the curves for the target events exceed one standard deviation. This indicates that regardless of the randomly chosen parameters, the epicenter of large target earthquakes has a reliably high PI percentile, which is caused by anomalous seismicity.

In the third test, we calculated the PI percentile for 10,000 random events using fixed (the red solid line in Fig. 11) and random (the red dot-dashed line in Fig. 11) PI parameters. Both cumulative distributions are nearly diagonal. These diagonal curves show that random samples are ergodic, in a statistical

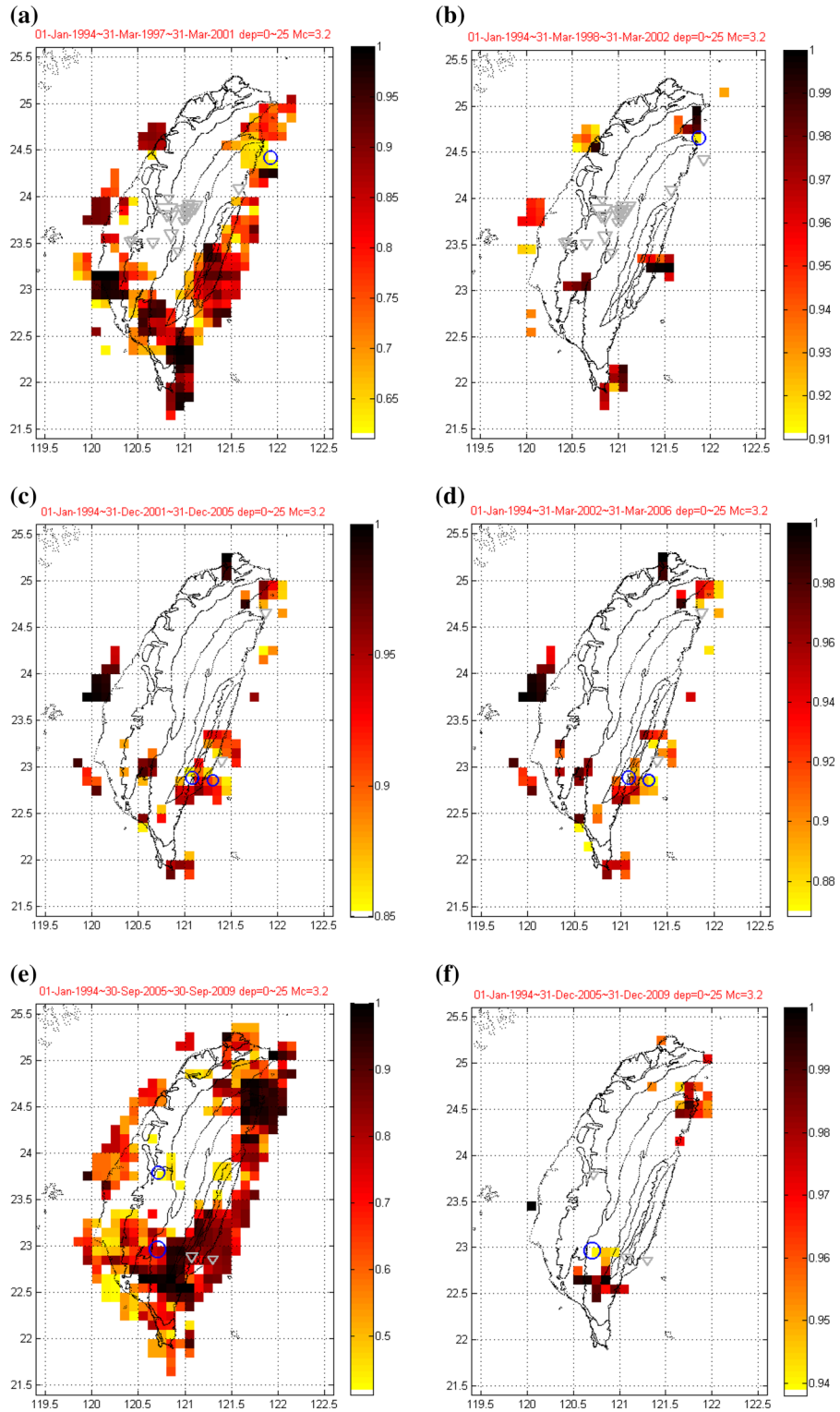


Figure 8

The hotspot map of the other target earthquakes by percentile. The hot spot map from **a** the first, **b** the second, **c** the fourth, **d** the fifth, **e** the sixth and **f** the seventh target event

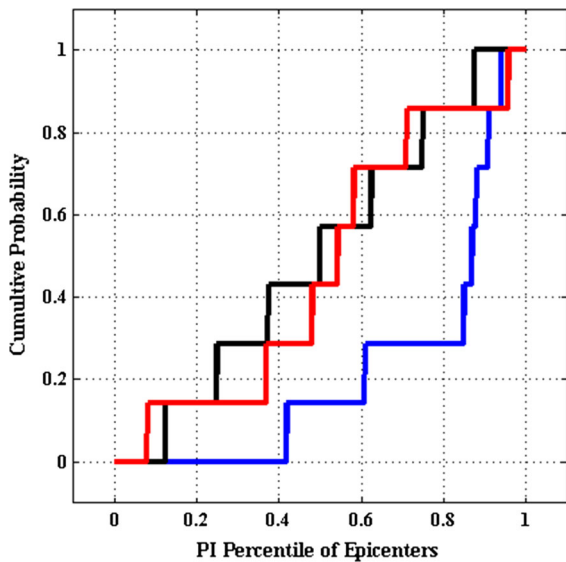


Figure 9

The cumulative probability of percentiles at given events. The *blue line* indicates the cumulative probability of percentile at the target events. The *black line* is the cumulative probability for 7 random events. The *red line* shows the cumulative probability of percentile for 7 target events from the re-calculated PI map with randomized seismicity given by the Poisson model

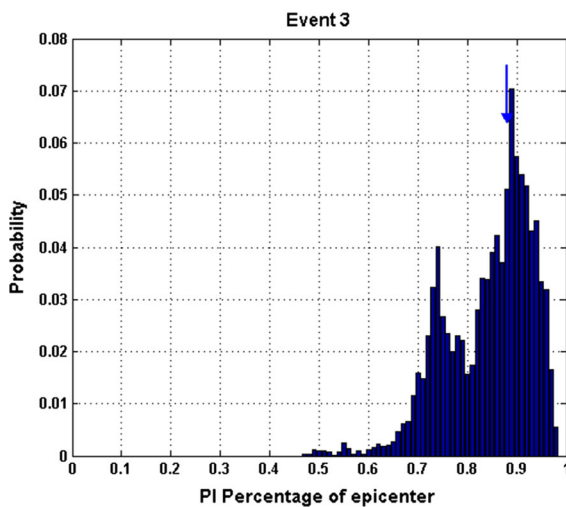


Figure 10

The probability distribution of the percentile for the Chengkung earthquake with random test parameters. We calculated the hotspot maps using 10,000 pairs of random parameters and counted the percentile at the epicenter in each map. The *blue arrow* indicates the result from the fixed parameters

sense (TIAMPO *et al.* 2010). However, the curves of the 7 target events, which are significantly different from the diagonal curves of the random samples,

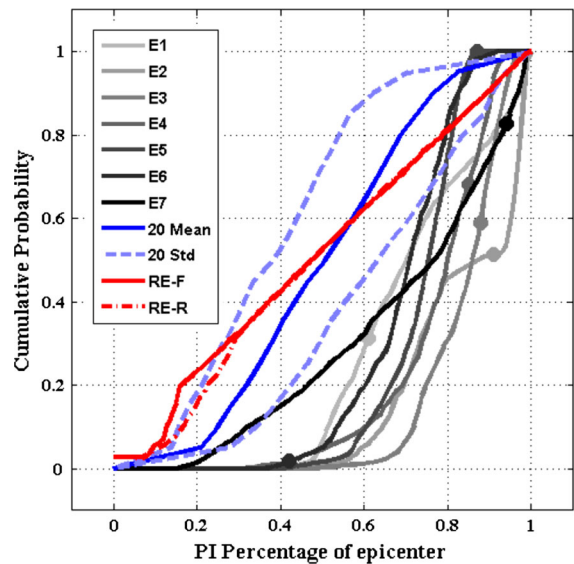


Figure 11

The cumulative probability of PI percentiles for 7 target events and 20 random events using 10,000 random PI parameter sets, and for 10,000 random events using fixed and random parameters. The lines (E1–E7) shown in *gray* and *black* indicate the cumulative probabilities of the PI percentiles for the 7 target events, and the *solid circle* on the line denotes the PI percentile of each event obtained from the PI hotspot map using the fixed parameters in Table 1. The *blue line* shows the mean of cumulative probabilities of the PI percentiles for the 20 random events, and the *dashed blue lines* show a range of one standard deviation. The *solid red line* (RE-F) and *dashed-dotted red line* (RE-R) are the cumulative probability distributions of 10,000 random events with fixed and random parameters, respectively

suggest that the epicenter area could experience a significant and reliable PI anomaly before large earthquakes.

6. Summary

In this study, we demonstrate how PI can be implemented to detect the likely epicenters of large earthquakes using a seasonal routine operation. Free parameters often and inevitably affect the performance in scientific simulations/predictions. In some cases, they can represent important physical meanings, and in other cases, simply mathematical tricks. In PI, the cutoff magnitude can be associated with the relationship between larger and smaller earthquakes, and the change interval with the time scale of nucleation processes of larger events. Nevertheless, they need to be assigned a priori for the routine operation.

For the PI parameters, we suggest a cutoff magnitude of 3.2 and a duration of change interval of 4 years. These values reveal anomalous seismic areas, which are typically associated with the forthcoming occurrence of $M > 6$ events in the Taiwan region. As demonstrated by the 7 targets listed in Table 1, the PI calculations with fixed parameters exhibit excellent potential for the epicenter detection of future large events. Although a visual inspection of the PI maps from the second random test does not produce clear precursory anomalies, statistical tests show that there is a precursory correlation. Furthermore, the statistical tests provide verification for the results of the routine operation. One drawback, which appeared in many PI hotspot maps, is the presence of many single and scattered patches. We regard these patches as noise, but they should be addressed in future studies.

Acknowledgments

The authors thank the Central Weather Bureau (CWB) for providing the earthquake data. CCC is grateful for research support from the Ministry of Science and Technology (ROC) and the Department of Earth Sciences at National Central University (ROC).

REFERENCES

- CHEN, C.-C., RUNDLE, J.B., HOLLIDAY, J.R., NANJO, K.Z., TURCOTTE, D.L., LI, S.C., and TIAMPO, K.F. (2005), *The 1999 Chi-Chi, Taiwan, earthquake as a typical example of seismic activation and quiescence*, *Geophys. Res. Lett.*, 32(22), L22315, doi:10.1029/2005GL023991.
- CHEN, C.-C., and WU, Y.X. (2006), *An improved region-time-length algorithm applied to the 1999 Chi-Chi, Taiwan earthquake*, *Geophys. J. Int.*, 166, 1144–1147.
- CHEN, C.-C., RUNDLE, J.B., LI, H.C., HOLLIDAY, J.R., NANJO, K.Z., TURCOTTE, D.L., and TIAMPO, K.F. (2006a), *From tornadoes to earthquakes: Forecast verification for binary events applied to the 1999 Chi-Chi, Taiwan, earthquake*, *Terr. Atmos. Ocean. Sci.*, 17, 503–516.
- CHEN, C.-C., RUNDLE, J.B., LI, H.C., HOLLIDAY, J.R., TURCOTTE, D.L., and TIAMPO, K.F. (2006b), *Critical point theory of earthquakes: Observation of correlated and cooperative behavior on earthquake fault systems*, *Geophys. Res. Lett.*, 33(18), L18302, doi:10.1029/2006GL027323.
- HOLLIDAY, J.R., CHEN, C.-C., TIAMPO, K.F., RUNDLE, J.B., TURCOTTE, D.L., and DONNELAN, A. (2007), *A RELM earthquake forecast based on pattern informatics*, *Seismol. Res. Lett.*, 78(1), 87–93.
- LEE, Y.T., TURCOTTE, D.L., HOLLIDAY, J.R., SACHS, M.K., RUNDLE, J.B., CHEN, C.-C., and TIAMPO, K.F. (2011), *Results of the Regional Earthquake Likelihood Models (RELM) test of earthquake forecasts in California*, *Proc. Natl. Acad. Sci. USA*, 108, 16533–16538, doi:10.1073/pnas.1113481108.
- LI, H.C., and CHEN, C.-C. (2011), *Characteristics of long-term regional seismicity before the 2008 Wen-chuan, China, earthquake using pattern informatics and genetic algorithms*, *Nat. Hazards Earth Syst. Sci.*, 11, 1003–1009.
- MIGNAN, A., WERNER, M.J., WIEMER, S., CHEN, C.-C., and WU, Y.M. (2011), *Bayesian estimation of the spatially varying completeness magnitude of earthquake catalogs*, *Bull. Seismol. Soc. Am.*, 101, 1371–1385.
- NANJO, K.Z., HOLLIDAY, J.R., CHEN, C.-C., RUNDLE, J.B., and TURCOTTE, D.L. (2006), *Application of a modified pattern informatics method to forecasting the locations of future large earthquakes in the central Japan*, *Tectonophysics*, 424, 351–366.
- RUNDLE, J.B., KLEIN, W., TIAMPO, K. and GROSS, S. (2000), *Linear Pattern Dynamics in Nonlinear Threshold Systems*, *Phys. Rev. E*, 61, 2418–2432.
- SCHORLEMMER, D., ZECHAR, J.D., WERNER, M.J., FIELD, E.H., JACKSON, D.D., JORDAN, T.H., and the RELM Working Group (Chen, C.-C. included) (2010), *First results of the Regional Earthquake Likelihood Models experiment*, *Pure Appl. Geophys.*, 167, 859–876.
- TIAMPO, K.F., RUNDLE, J.B., MCGINNIS, S., GROSS, S.J. and KLEIN, W. (2002), *Mean-field threshold systems and phase dynamics: An application to earthquake fault systems*, *Europhys. Lett.*, 60(3), 481–487.
- TIAMPO, K.F. and SHCHERBAKOV, R. (2012), *Seismicity-based earthquake forecasting techniques: Ten years of progress*, *Tectonophysics*, Volumes 522–523, 89–121.
- TIAMPO, K.F., KLEIN, W., LI, H.C., MIGNAN, A., TOYA, Y., KOHEN-KADOSH, S.Z.L., RUNDLE, J.B., and CHEN, C.-C. (2010), *Ergodicity and earthquake catalogs: Forecast testing and resulting implications*, *Pure Appl. Geophys.*, 167, 763–782.
- TOYA, Y., TIAMPO, K.F., RUNDLE, J.B., CHEN, C.-C., LI, H.C., and KLEIN, W. (2010), *Pattern informatics approach to earthquake forecasting in 3D*, *Concurrency and Computation Practice and Experience*, 22, 1569–1592.
- WU, Y.H., CHEN, C.-C., and RUNDLE, J.B. (2008a), *Detecting precursory earthquake migration patterns using the pattern informatics method*, *Geophys. Res. Lett.*, 35, L19304, doi:10.1029/2008GL035215.
- WU, Y.H., CHEN, C.-C., and RUNDLE, J.B. (2008b), *Precursory seismic activation of the Pingtung (Taiwan) offshore doublet earthquakes on 26 December 2006: A pattern informatics analysis*, *Terr. Atmos. Ocean. Sci.*, 19, 743–749.
- WU, Y.H., CHEN, C.-C., and RUNDLE, J.B. (2011), *Precursory small earthquake migration patterns*, *Terra Nova*, 23, 369–374.
- WU, Y.M., and CHIAO, L.Y. (2006), *Seismic quiescence before the 1999 Chi-Chi, Taiwan, M_w 7.6 earthquake*, *Bull. Seism. Soc. Am.*, 96(1), 321–327.